JOM, Vol. 69, No. 11, 2017
DOI: 10.1007/s11837-017-2461-0

Unique Challenges for Modeling Defect Dynamics in Concentrated Solid-Solution Alloys

SHIJUN ZHAO,[1,3] WILLIAM J. WEBER,[1,2,4] and YANWEN ZHANG[1,2,5]

1.—Materials Science and Technology Division, Oak Ridge National Laboratory, Oak Ridge, TN 37831, USA. 2.—Department of Materials Science and Engineering, University of Tennessee, Knoxville, TN 37996, USA. 3.—e-mail: zhaos@ornl.gov. 4.—e-mail: wjweber@utk.edu. 5.—e-mail: zhangy1@ornl.gov

Recently developed concentrated solid solution alloys (CSAs) are shown to have improved performance under irradiation that depends strongly on the number of alloying elements, alloying species, and their concentrations. In contrast to conventional dilute alloys, CSAs are composed of multiple principal elements situated randomly in a simple crystalline lattice. As a result, the intrinsic disorder has a profound influence on energy dissipation pathways and defect evolution when these CSAs are subjected to energetic particle irradiation. Extraordinary irradiation resistance, including suppression of void formation by two orders of magnitude at an elevated temperature, has been achieved with increasing compositional complexity in CSAs. Unfortunately, the loss of translational invariance associated with the intrinsic chemical disorder poses great challenges to theoretical modeling at the electronic and atomic levels. Based on recent computer simulation results for a set of novel Ni-containing, face-centered cubic CSAs, we review theoretical modeling progress in handling disorder in CSAs and underscore the impact of disorder on defect dynamics. We emphasize in particular the unique challenges associated with the description of defect dynamics in CSAs.

INTRODUCTION

In contrast to conventional dilute alloys, recently developed concentrated solid solution alloys (CSAs), including high-entropy alloys (HEAs), contain multiple principal elements situated in a simple lattice at or near equiatomic concentrations.[1] This new type of alloys is characterized by a disordered state related to random arrangement of different chemical element species and associated random displacement fluctuations. It has been demonstrated, both experimentally and theoretically, that many properties of CSAs are closely related to the underlying disordered state.[2–5] Although it is observed that these compositionally complex alloy systems display a significant resistance to radiation damage (such as the suppression of void formation by two orders of magnitude at high temperatures[6]), little is known about the controlling elemental or chemical effects in these homogeneously disordered alloys concerning their local heterogeneity at the electronic and atomic levels.[5] In particular, depending on the chemical complexities, distinct irradiation-resistant properties are observed in different CSAs.[3–7] Therefore, it is anticipated that the energy dissipation pathways and defect kinetics are strongly affected by the disordered state in CSAs. Accordingly, understanding the role of chemical disorder under the far-from-equilibrium conditions associated with displacement cascades is becoming one of the most critical problems in the development of irradiation-resistant CSAs.

Here, the unique challenges related to the modeling of the defect dynamics in CSAs are reviewed. The focus will be on the most widely studied Ni-

This manuscript has been authored by UT–Battelle, LLC under Contract No. DE–AC05–00OR22725 with the U.S. Department of Energy. The publisher, by accepting the article for publication, acknowledges that the U.S. Government retains a nonexclusive, paid-up, irrevocable, worldwide license to publish or reproduce the published form of this article, or to allow others to do so, for U.S. Government purposes. The Department of Energy will provide public access to these results of federally sponsored research in accordance with the DOE Public Access Plan.

(Published online July 20, 2017)

containing, face-centered-cubic (*fcc*) CSAs. Special attention is paid to the effect of intrinsic disorder in CSAs on defect kinetics at the electronic and atomic levels. In reviewing recent progress in this field, the range of theoretical methods employed to overcome the challenges caused by the disordered state in CSAs are considered in detail, and the implications and limitations of these theoretical approaches are discussed.

DEFECT PROPERTIES

Under ion irradiation, the energy of incident energetic ions is transferred to electrons and atomic nuclei in the target, which creates defects.[5] Thus, it is important to characterize defect energies and the associated defect stabilities.

Defect Energetics

Because of the unique disordered state in CSAs, defect formation energies and migration energies are strongly dependent on local environments. As a result, the defect energies in CSAs exhibit distributions rather than some specific values, as in pure metals or dilute alloys. To characterize the defect energetics in CSAs, a large dataset is required to represent the distributions of atomic environments. Although ab initio methods based on density functional theory (DFT) have become standard approaches to investigate defect energies, the disordered states in CSAs pose great challenges to such modeling efforts.

Nowadays, three widely used techniques are usually employed to address the disorder-related problems: the coherent potential approximation (CPA),[8] the special quasi-random structures (SQS) method,[9] and the cluster expansion (CE) approach.[10] The CPA method takes the effect of chemical and magnetic disorder on the configurationally averaged electronic structure of disordered alloys into account elegantly. Nevertheless, the single-site or mean-field nature of CPA limits its applicability because local lattice relaxations are neglected in this scheme. Regarding defect energetics in disordered alloys, the CPA method is best applied to study the formation energy of defects that do not induce strong local structural relaxations, such as vacancies.[11,12] This method can describe defect energies efficiently under different alloy concentrations.[11] Nevertheless, the distribution of defect energies in CSAs, which depends on local atomic arrangements, cannot be obtained within CPA. In addition, the CPA-based methods cannot describe defect migration directly. Future development of a nonlocal CPA method[13] may enable the consideration of local effects, but at present, one has to resort to supercell-based approaches, i.e., the so-called SQS method. The SQS approach is designed to simulate a random alloy using a small periodic supercell that mimics the most relevant radial correlation functions of the random alloy. Based on SQS, the defect formation and migration energies, and the associated local lattice distortions can be modeled directly by first-principles methods. Hence, this method is suitable for describing defect energy distributions in CSAs.[14] The main disadvantage of this method is the high computational cost because a large supercell must be employed to minimize the spurious interactions induced by defects in the periodic images. In addition, lots of defect configurations must be considered to obtain an overall picture of defect energetics. Finally, the CE method is powerful for predicting the energy of specific atomic configurations in a simple lattice using the knowledge of the energies for a small number of configurations. For defect-free systems, typically 30–50 configurations are enough to obtain converged results. For defect calculations, defects such as vacancies and interstitials are usually considered to be additional species.[15,16] As a result, the parametrization becomes computationally expensive for multicomponent alloys. At present, only the defect properties in binary alloys have been studied using this method.[15,16]

Within the SQS supercell method, defects such as vacancies and interstitials can be modeled by adding or removing specific atomic elements. The formation energy of a defect type α is calculated by $E_f(\alpha) = E_T(\alpha) - E_0 \pm \mu_\alpha$, where $E_T(\alpha)$ is the total energy of the supercell containing the defect, E_0 is the total energy of the defect-free supercell, and μ_α is the chemical potential of the defect species α that is added to (−) or removed from (+) the perfect lattice. Although the first two terms can be calculated directly based on first-principles methods, the elemental chemical potential depends strongly on the local environment in CSAs. Experimentally, μ is related to the specific growth conditions. For a pure metal, μ is usually taken to be the energy per atom in the metal. In previous studies, μ in disordered alloys has also been taken as the energy in the corresponding pure metal as the reference:[17–19] $\mu_\alpha = \mu_\alpha^{bulk}$. Nevertheless, in reality, it is highly likely that μ in the alloy phase is different from those in the corresponding pure metal. Indeed, Middleburgh et al.[19] have studied the defect properties in NiCoFeCr CSA using the pure metals as chemical potential references and obtained numerous negative vacancy formation energies. The determination of μ in CSAs is beginning to receive increasing attention. In view of the thermodynamic consideration, Piochaud et al.[14] have suggested that the chemical potential difference of different elements at 0 K can be approximated by the minimum of substitution energy. From the alloy stability point of view, Zhao et al.[20] have proposed an efficient way to average the substitutional energy. These methods provide insight into the chemical potential of different elements in the alloy phase. In the CE formalism, the chemical potentials of different elements

can be extracted by fitting the mixing enthalpy as a function of different alloy compositions, as demonstrated by Zhang et al.[15]

Based on the SQS supercell model, it is shown that the formation energy of intrinsic point defects, such as vacancies and interstitials in CSAs, is widely distributed.[14,19–21] In particular, Piochaud et al.[14] have showed that the energies can be fitted using variables describing the local environment surrounding the defect. The results show that the dominant factor in determining defect energies is the first nearest-neighbor shell. In the Ni-containing CSAs, including $Ni_{0.5}Co_{0.5}$, $Ni_{0.5}Fe_{0.5}$, $Ni_{0.8}Fe_{0.2}$, and $Ni_{0.8}Cr_{0.2}$, the formation energies of vacancies tend to decrease as the number of nearest Ni neighbors increases.[20] The distribution of defect energies is found to exhibit different features in these CSAs. As an illustration, the distributions of formation energies for vacancies and interstitials are provided in Fig. 1. These defects are modeled by removing (vacancies) or adding (interstitials) one specific element into the perfect SQS cell. In $Ni_{0.5}Co_{0.5}$, it is shown that the formation energies of Ni and Co vacancies are very similar. In both $Ni_{0.5}Fe_{0.5}$ and $Ni_{0.8}Fe_{0.2}$, Fe vacancies exhibit lower formation energies than do Ni vacancies. In $Ni_{0.8}Cr_{0.2}$, the formation energies of Cr vacancies are lower than those of Ni vacancies. For interstitials, Fig. 1 demonstrates that Co–Co and Co–Ni dumbbell interstitials have lower formation energies than Ni–Ni does in $Ni_{0.5}Co_{0.5}$. The formation energies of Ni–Fe and Ni–Ni are lower than Fe–Fe is in both $Ni_{0.5}Fe_{0.5}$ and $Ni_{0.8}Fe_{0.2}$. Ni–Cr dumbbell interstitials are more energetically favorable in $Ni_{0.8}Cr_{0.2}$. Compared with the defect properties in pure Ni, it can be seen that the formation energies of vacancies are mostly higher than those in pure Ni, whereas the formation energies of interstitials are lower, especially in $Ni_{0.5}Fe_{0.5}$. This observation suggests that the energy differences in creating vacancy and interstitial defects in CSAs become much smaller.

Defect energies are closely related to defect stabilities. Nevertheless, most ab initio methods used to study defect energies are carried out at 0 K. To investigate defect thermodynamics more relevant to the experiment, the Gibbs free energy of defect formation should be calculated. The defect formation free energy includes the contribution from configurations, electrons, phonons, and magnons. The configurational entropy is attributed to the possible random positions of defects. Usually, the electronic free energy can be calculated from the electronic density of states, while the phonon contribution is obtained from the phonon density of states (quasi-harmonic approximation in most cases). It is, however, not apparent how to tackle magnetic free energy within supercell methods. For CSAs, the determination of these terms is difficult because of the wide distribution of defect energies. Although calculations have been performed in pure metals to analyze the entropy contribution to the vacancy formation,[22,23] there are currently no reports for CSAs. Note that CPA and CE methods have been further developed to study the temperature dependence of vacancy formation energies in random alloys.[15,24,25]

Another critical issue for CSA modeling using ab initio methods is their complex magnetic properties. Although the lattice structure of CSAs is simple, their magnetic properties can vary from ferromagnetic (FM) to antiferromagnetic (AFM) to paramagnetic (PM). In particular, some elements such as Mn exhibit frustrated magnetism in CSAs because of the disordered neighboring magnetic state. Their magnetic moments cannot align optimally according to the local environment, e.g., unable to align optimally to either part of coordination to make it in definite AFM or FM state. For the Ni–Co, Ni–Fe, and Ni–Cr CSAs presented earlier, it is less problematic because these CSAs are either FM or AFM. For the PM state in some CSAs, such as NiCoFeCr,[26] the disordered local moment (DLM) approximation[27] is usually employed. In this scheme, a PM state is modeled by an equal number of spin-up and spin-down atoms randomly distributed on the underlying sublattice. For example, PM NiCoFeCr is described by Ni(↑)Ni(↓)Co(↑)Co(↓)-Fe(↑)Fe(↓)Cr(↑)Cr(↓) with eight species. The increased number of elemental species leads to additional complexity for ab initio calculations.

Defect Migration

The migration of defects is important for understanding of microscopic evolution under ion irradiation. At 0 K, the ab initio climbing-image nudged elastic band (CI-NEB) method[28] is usually used to calculate migration barriers and associated diffusion paths. In such calculations, the initial and final states of the diffusion path are fixed and the diffusion pathway is prespecified by interpolating several images between the two known states. In *fcc* Ni, the most preferable diffusion pathway for a [100] dumbbell interstitial is to transform into a [010] dumbbell by a rotating mechanism.[29] Based on the same mechanism, Zhao et al.[20] studied the diffusion in CSAs using the NEB calculations. Depending on the local environment, the migration barriers in CSAs also exhibit distributions. It is found that the migration barriers of interstitials in Ni-containing binary CSAs are mostly higher than those in pure Ni, an indication of sluggish diffusion of interstitials.[20] This fact can be traced back to the lower formation energy of interstitials, as discussed in the previous section, which leads to strong binding interactions between interstitial and lattice atoms.

The NEB calculations require prior knowledge of the final state for a specific defect type. In addition, it is difficult to get an overall diffusion behavior of defects even if all possible diffusion barriers are studied exhaustively using NEB methods.

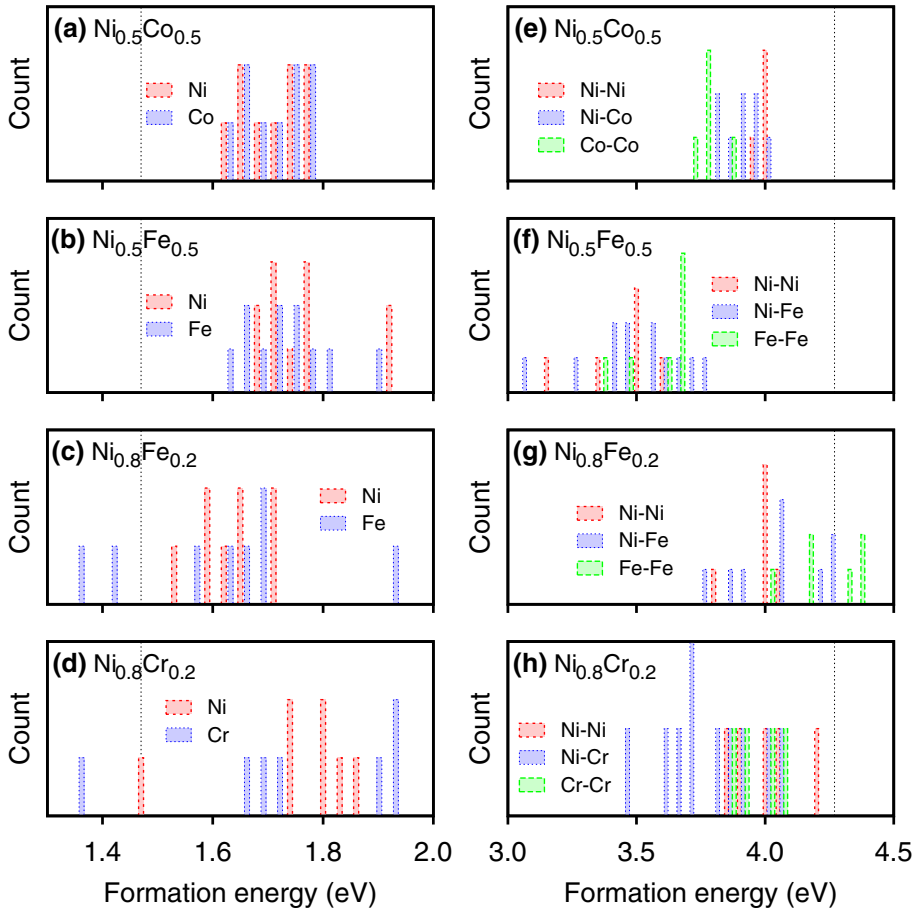

Fig. 1. Distribution of formation energies for vacancies (left column) and interstitials (right column) in $Ni_{0.5}Co_{0.5}$ (a and e), $Ni_{0.5}Fe_{0.5}$ (b and f), $Ni_{0.8}Fe_{0.2}$ (c and g), and $Ni_{0.8}Cr_{0.2}$ (d and h) calculated from a 108-atom SQS supercell model. The formation energy in pure Ni is denoted by dashed lines for both vacancies and interstitials. The number of data points used for the plot is around 15–25. Adapted from Ref. 20.

Furthermore, the temperature effect is usually ignored in such calculations. To allow the defect to migrate according to the local energy landscape in CSAs, it is better to perform molecular dynamics (MD) simulations. In this way, the defect can find its optimal diffusion pathway according to the local potential energy profile at different temperatures.

Both ab initio MD (AIMD) and classic MD (CMD) simulations have been carried out to investigate the specific features of diffusion in CSAs.[30–33] These two methods have strengths and weaknesses regarding the diffusion problem. For the AIMD method, it can provide accurate energy and force at the quantum mechanics level; thus, the energy landscape can be described accurately without any model constraint. Nevertheless, the description of electronic interactions comes at a high computational cost. As a consequence, the simulation cell size and simulation time are limited for this method. For diffusion processes, which are basically a statistical problem, significant numbers of defect jumps must be simulated to calculate diffusion coefficients accurately. Therefore, this method is more often used to study the diffusion of interstitial defects because the diffusion of interstitials is much faster. Nevertheless, in CSAs, the diffusion of interstitials is slower than that in pure metals, as revealed by static NEB calculations. This leads to further difficulty in studying the diffusion problem with AIMD. For the CMD method, the diffusion trajectory can be simulated for a long time (in $\sim\mu$s time frame). Yet the results of CMD depend sensitively on the interatomic potentials employed.

The simulation results from both AIMD and CMD suggest that there is preferential diffusion of point defects belonging to particular constituent components in CSAs. Osetsky et al.[30] showed that the diffusion of interstitials in NiFe is mainly through the Ni channel, whereas the diffusion of vacancies in NiFe is mainly via the Fe channel. The fact that the migration of interstitials and vacancies is through different alloy components suggests unique mass transport pathways in CSAs. These observations can be tracked back to the defect formation energy distributions. As shown in Fig. 1, lower formation energies are found predominantly for Ni–Ni and Ni–Fe dumbbell interstitials and for Fe vacancies. These preferred defect structures determine defect flow when defect diffusion begins.[33] Therefore, to use CMD to study defect diffusion in

CSAs, it is important to compare the defect energetics predicted by the empirical potentials with ab initio results to ensure that the interatomic potentials reproduce the correct defect energetics.

The local environment-dependent migration barriers in CSAs are especially important as necessary inputs for large-scale simulations, such as kinetic Monte Carlo (KMC) methods. To this end, various approaches trying to correlate migration barriers with the local atomic environment have been proposed. In CSAs, the local environment can be complex and enumeration-based methods are not practical. The artificial neural network (ANN) technique[34–36] constructs a mathematical regression of the NEB energy barrier with respect to local environment. Based on a small training dataset, this method is capable of predicting migration barriers under an arbitrary local environment,[34] which is useful in practical KMC simulations.

DEFECT DYNAMICS

Primary Damage

Under irradiation, the energy transferred from the incident ions to the target leads to defect production. One of the basic quantities determining the defect production in materials is the threshold displacement energy (E_d), which is the minimal energy required to displace an atom from its original lattice position and create a stable defect. In pure metals, CMD has been used extensively to investigate E_d values and associated low-energy recoil events, including defect dynamics and defect properties.[37–39] Some CMD studies also have been performed to calculate E_d in solid solution alloys.[40,41] Although the results from such calculations depend on the quality of the interatomic potentials, significant insight has been gained from these studies.

To overcome the limitation of empirical potentials used in CMD calculations, AIMD has been employed to investigate E_d in CSAs. The disorder inherent in CSAs leads to difficulty in determining E_d even in one specific primary knocked-on atom (PKA) direction. For NiCo, Liu et al. studied the alloying effects on the values of E_d using a simple model to consider the chemical disorder.[42] The model corresponds to some extreme cases (ordered arrangement of elements), and the boundaries of E_d from pure metals to totally disordered CSAs may be revealed. In practice, both the chemical disorder and the displacement fluctuation should be taken into account. By equilibrating the system for a long time before assigning certain kinetic energy to the PKA, these two factors can be considered simultaneously. It is found that E_d in CSAs exhibits a distribution depending on the local environment because of elemental variation. As an illustration, Fig. 2 shows the trajectories of low-energy recoil events initiated by three randomly chosen Fe PKAs along the [111] direction in NiFe. Note that the atoms are slightly deviated from the lattice sites. In a *fcc* structure, the {111} planes are closely packed. As a result, the PKA must pass through two adjacent close-packed planes before its head-on collision with an atom in the [111] direction, as indicated by the arrow in Fig. 2. In NiFe, the disorder significantly changes the PKA trajectories so that the PKA may change directions when it passes through the second neighbor plane, as shown in Fig. 2a and c. Accordingly, the value of E_d determined in each case is different. To characterize the distribution of E_d and the according defect production, many environmentally independent, low-energy recoil events need to be simulated, which is a challenge for the computationally intensive AIMD calculations. It should be noted that the Born–Oppenheimer and frozen core approximation may lead to some uncertainties in such collision simulations.

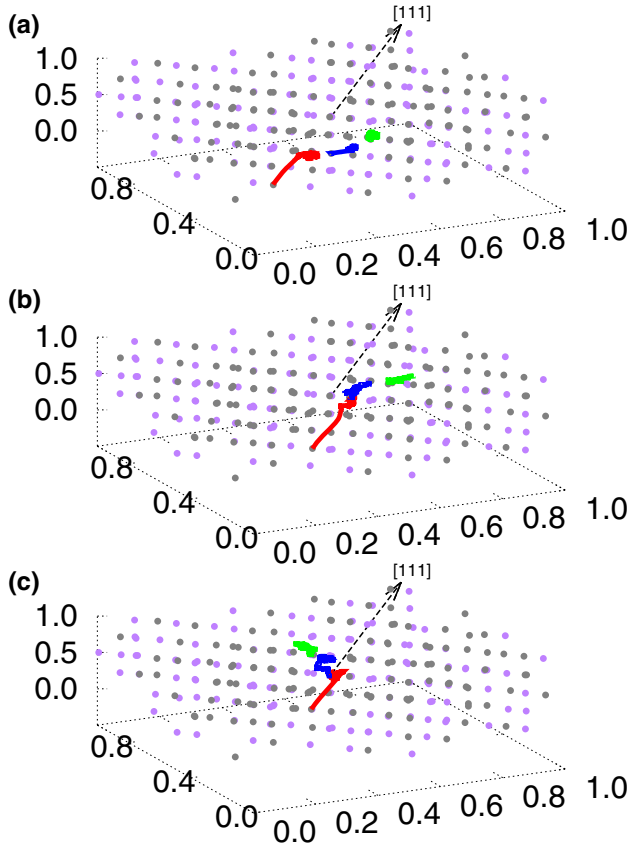

Fig. 2. Three trajectories (a, b and c) of low-energy recoil events in NiFe initiated by three different Fe PKAs obtained from a 256-atom SQS supercell. The numerical details are the same as those in Ref. 42. Ni and Fe atoms are denoted by purple and gray dots, respectively. Only the trajectories for those atoms with a displacement of larger than 1 Å are plotted.

For collision cascades induced by keV-energy ion irradiation, simulations at longer times and length scales than AIMD must be employed. In this regard, CMD has been employed widely to study defect production and accumulation in CSAs.[3,4,7,43–46] These results consistently show that alloying of Ni

with Fe, Co, and Cr tends to reduce the primary damage accumulation under ion irradiation, although different elements yield different damage accumulation levels. In addition, different defect structures in Ni and its CSAs are revealed: Large defect clusters are produced in pure Ni, whereas smaller defect clusters with higher number densities are formed in CSAs. Nevertheless, the mechanism responsible for the reduced damage in CSAs is not clear. In a recent work, Levo et al.[46] showed that there is a correlation between damage level in different alloys and dislocation mobilities. Note that the damage in these alloys induced by a single 5-keV cascade is not much different from that produced in pure Ni.[5] Based on these simulations, it is indicated that the potential energy landscape of CSAs favors efficient recombination of interstitial and vacancy defects because the subcascades in Ni and its CSAs exhibit similar energies and spatial distributions. Hence, the details of the defect energy landscape in CSAs are of significant importance to understand their irradiation performance. Although specific features are revealed in these simulations, the results and conclusions are dependent on the empirical potentials used. A typical example is the much different defect number created in NiFe as a result of 10- to 40-keV displacement cascades with different empirical potentials, as demonstrated by Béland et al.[43]

For even higher energy ion irradiation, it is supposed that electronic effects should come into play. Indeed, simulation results from the two-temperature model by Zarkadoula et al.[47] suggest that the damage level and defect configurations in Ni and NiFe are significantly affected by including electronic effects even in 50-keV casacades. In such high-energy events, the energy exchange between electrons and phonons plays an important role in governing defect evolution. Therefore, accurate determinations of model parameters are necessary to address the problem in full.

Long-Term Evolution

The evolution of defects produced by ion irradiation has direct relevance to the microstructure change in materials. To gain insight into defect evolution in CSAs, CMD is carried out by randomly adding defects into simulation cells.[6,48,49] In this way, longer simulation times can be simulated and the nature of defect migration and diffusion can be captured effectively. Yet because of the limited simulation cell sizes employed in this method, the concentration of defects is usually much higher than that observed experimentally. Nevertheless, this approach is effective in reproducing the experimentally observed defect clusters and in revealing the underlying evolution mechanisms.

The evolution of both point defects and defect clusters has been studied using this method. Aidhy et al.[48] found that interstitials mainly form $1/3\{111\}\langle 111\rangle$ dislocation loops, whereas vacancies form stacking fault tetrahedra. In addition, larger size defect clusters are formed in pure Ni, whereas clusters of smaller size and larger numbers are observed in the CSAs. Lu et al.[6] showed that the diffusion of small interstitial clusters in some CSAs is through a three-dimensional (3D) short-range fashion, in contrast to the one-dimensional (1D) long-range migration in pure Ni and NiCo. The results suggest enhanced void swelling resistance in CSAs because the 3D migration of interstitial clusters can lead to increasing recombination between vacancies and interstitials. Zhao et al.[49] have simulated the diffusion of vacancy clusters in various CSAs and demonstrated that the diffusion coefficients of small vacancy clusters in CSAs are higher than in pure Ni, whereas the diffusion coefficients become lower for large vacancy clusters. This observation suggests that large clusters can easily migrate and grow to very large sizes in pure Ni. In contrast, cluster growth is suppressed in solid solution alloys as a result of the limited mobility of large vacancy clusters. The motion of dislocations in *bcc* and *fcc* CSAs is also studied by CMD simulations, which demonstrate consistently a strengthening effect in CSAs because of the local variation in composition along dislocation lines.[50,51] The variation leads to a distribution of the local stacking fault energy, making the dislocation motion unfavorable.

The simulation time in CMD is limited from the nanosecond to microsecond time scales. To access longer time scale processes associated with defect evolution, MC methods, such as KMC and kinetic activation relaxation technique (k-ART),[52] are usually employed. These MC techniques rely on the prior knowledge on the defect parameters, including defect formation energies, migration barriers, and defect jump frequencies. These parameters must be calculated in advance using interatomic potentials, ab initio techniques, or on-the-fly barrier calculations.[53] As discussed, the defect energies in CSAs exhibit distributions depending on local environment, which creates a challenge in determining the input required for MC simulations. As long as the defect energies are known, the MC technique can simulate defect evolution up to more than one second time scale. Such calculations have been used to study the aging of defects between cascade events at room temperature.[4,54–57]

MULTISCALE MODELING OF DAMAGE EVOLUTION

The damage evolution under ion irradiation is a typical multiscale problem. Starting from the electronic and atomic levels, DFT and MD methods can be used to study defect production, evolution, and defect interactions, which provide information on the thermodynamics and kinetics of defect or defect clusters within various environments. Based on the established defect energetics, KMC is capable of

long simulations about the defect evolution. Finally, the continuum approaches can be employed to probe the changes in microstructures, as well as in the mechanical properties, that ultimately lead to the material degradation. This hierarchical multiscale computational framework has been extensively used to study materials properties under ion irradiation.[58]

For CSAs, various difficulties are associated with these individual techniques. In addition, it is difficult to provide the linkage among these different methods from local processes to larger scale evolutions because of the strong dependence of defect properties on the local environment. To construct a catalog accurately for all the configurations would be cumbersome. Therefore, efficient methods, such as ANN techniques that enable on-the-fly calculation of migration barriers, are promising,[34] and these methods have been used to model radiation damage in Fe–Cr[59] and related alloys.[60] For CSAs, such methods are extremely important because the local environment dependence can be reasonably taken into account. Multiscale modeling is necessary to reveal the mechanistic understanding and to establish semi-empirical models for material aging and irradiation-induced property degradation in CSAs.

SUMMARY

Although computer simulations have been employed extensively to study defect production and evolution in pure metals and conventional dilute alloys, the recently developed CSAs pose great challenges to these widely used simulation techniques. Specifically, the intrinsic chemical disorder and associated displacement fluctuations within CSAs must be taken into account properly to capture the defect properties in CSAs. As defect behaviors depend sensitively on local environments, it is necessary to include the structure details in the calculations explicitly. In CSAs, the randomness of local environments leads to wide distributions of defect-related properties rather than to definitive values. Taking into account the presence of these distributions is vital to understanding the irradiation performance of CSAs. Therefore, a large sampling effort is required to get an overall picture of defect behavior. Although MD and MC methods enable exhaustive exploration of local environments using large cell sizes and long simulation times, these methods are limited by the availability and quality of empirical potentials. Overcoming these challenges and fully understanding the energy dissipation and defect evolution mechanisms is the key to establishing the relationship between the underlying disordered state and improved irradiation performance in CSAs.

ACKNOWLEDGEMENT

This work was supported as part of the Energy Dissipation to Defect Evolution (EDDE), an Energy Frontier Research Center funded by the U.S. Department of Energy, Office of Science, Basic Energy Sciences.

REFERENCES

1. M.-H. Tsai and J.-W. Yeh, *Mater. Res. Lett.* 2, 107 (2014).
2. K. Jin, B.C. Sales, G.M. Stocks, G.D. Samolyuk, M. Daene, W.J. Weber, Y. Zhang, and H. Bei, *Sci. Rep.* 6, 20159 (2016).
3. Y. Zhang, G.M. Stocks, K. Jin, C. Lu, H. Bei, B.C. Sales, L. Wang, L.K. Béland, R.E. Stoller, G.D. Samolyuk, M. Caro, A. Caro, and W.J. Weber, *Nat. Commun.* 6, 8736 (2015).
4. Y. Zhang, K. Jin, H. Xue, C. Lu, R.J. Olsen, L.K. Beland, M.W. Ullah, S. Zhao, H. Bei, D.S. Aidhy, G.D. Samolyuk, L. Wang, M. Caro, A. Caro, G.M. Stocks, B.C. Larson, I.M. Robertson, A.A. Correa, and W.J. Weber, *J. Mater. Res.* 31, 2363 (2016).
5. Y. Zhang, S. Zhao, W.J. Weber, K. Nordlund, F. Granbergc, and F. Djurabekova, *Curr. Opin. Solid State Mater. Sci.* (2017). doi:10.1016/j.cossms.2017.02.002.
6. C. Lu, L. Niu, N. Chen, K. Jin, T. Yang, P. Xiu, Y. Zhang, F. Gao, H. Bei, S. Shi, M.-R. He, I.M. Robertson, W.J. Weber, and L. Wang, *Nat. Commun.* 7, 13564 (2016).
7. F. Granberg, K. Nordlund, M.W. Ullah, K. Jin, C. Lu, H. Bei, L.M. Wang, F. Djurabekova, W.J. Weber, and Y. Zhang, *Phys. Rev. Lett.* 116, 135504 (2016).
8. B.L. Gyorffy, *Phys. Rev. B* 5, 2382 (1972).
9. A. Zunger, S.-H. Wei, L.G. Ferreira, and J.E. Bernard, *Phys. Rev. Lett.* 65, 353 (1990).
10. J.M. Sanchez, F. Ducastelle, and D. Gratias, *Phys. A Stat. Mech. Its Appl.* 128, 334 (1984).
11. L. Delczeg, B. Johansson, and L. Vitos, *Phys. Rev. B* 85, 174101 (2012).
12. E.K. Delczeg-Czirjak, L. Delczeg, L. Vitos, and O. Eriksson, *Phys. Rev. B* 92, 224107 (2015).
13. J.B. Staunton, D.D. Johnson, and F.J. Pinski, *Phys. Rev. B* 50, 1450 (1994).
14. J.B. Piochaud, T.P.C. Klaver, G. Adjanor, P. Olsson, C. Domain, and C.S. Becquart, *Phys. Rev. B* 89, 24101 (2014).
15. X. Zhang and M.H.F. Sluiter, *Phys. Rev. B* 91, 174107 (2015).
16. A. Van Der Ven and G. Ceder, *Phys. Rev. B* 71, 54102 (2005).
17. M. Muzyk, D. Nguyen-Manh, K.J. Kurzydłowski, N.L. Baluc, and S.L. Dudarev, *Phys. Rev. B* 84, 104115 (2011).
18. E. Del Rio, J.M. Sampedro, H. Dogo, M.J.M.J. Caturla, M. Caro, A. Caro, and J.M. Perlado, *J. Nucl. Mater.* 408, 18 (2011).
19. S.C. Middleburgh, D.M. King, G.R. Lumpkin, M. Cortie, and L. Edwards, *J. Alloys Compd.* 599, 179 (2014).
20. S. Zhao, G.M. Stocks, and Y. Zhang, *Phys. Chem. Chem. Phys.* 18, 24043 (2016).
21. J.S. Wróbel, D. Nguyen-Manh, S.L. Dudarev, and K.J. Kurzydłowski, *Nucl. Instrum. Methods Phys. Res. Sect. B Beam Interact. Mater. Atoms* 393, 126 (2017).
22. A. Glensk, B. Grabowski, T. Hickel, and J. Neugebauer, *Phys. Rev. X* 4, 11018 (2014).
23. A. Metsue, A. Oudriss, J. Bouhattate, and X. Feaugas, *J. Chem. Phys.* 140, 104705 (2014).
24. A.V. Ruban, *Phys. Rev. B* 93, 134115 (2016).
25. H.B. Luo, Q.M. Hu, J. Du, A.R. Yan, and J.P. Liu. arXiv preprint https://arxiv.org/abs/1702.03104 (2017).
26. M.S. Lucas, L. Mauger, J.A. Muñoz, Y. Xiao, A.O. Sheets, S.L. Semiatin, J. Horwath, and Z. Turgut, *J. Appl. Phys.* 109, 07E307 (2011).
27. F.J. Pinski, J. Staunton, B.L. Gyorffy, D.D. Johnson, and G.M. Stocks, *Phys. Rev. Lett.* 56, 2096 (1986).
28. G. Henkelman, B.P. Uberuaga, and H. Jónsson, *J. Chem. Phys.* 113, 9901 (2000).
29. J.D. Tucker, T.R. Allen, and D. Morgan, *13th Environmental Degradation of Materials in Nuclear Power System* (2007).
30. Y.N. Osetsky, L.K. Béland, and R.E. Stoller, *Acta Mater.* 115, 364 (2016).

31. L. Barnard and D. Morgan, *J. Nucl. Mater.* 449, 225 (2014).
32. J.D. Tucker, R. Najafabadi, T.R. Allen, and D. Morgan, *J. Nucl. Mater.* 405, 216 (2010).
33. S. Zhao, Y. Osetsky, and Y. Zhang, *Acta Mater.* 128, 391 (2017).
34. N. Castin and L. Malerba, *J. Chem. Phys.* 132, 74507 (2010).
35. G. Bonny, N. Castin, and D. Terentyev, *Model. Simul. Mater. Sci. Eng.* 21, 85004 (2013).
36. D. Terentyev, N. Castin, and C.J. Ortiz, *J. Phys. Condens. Matter* 24, 475404 (2012).
37. A.J.E. Foreman, C.A. English, and W.J. Phythian, *Philos. Mag. A* 66, 655 (1992).
38. D. Bacon, Y. Osetsky, R. Stoller, and R. Voskoboinikov, *J. Nucl. Mater.* 323, 152 (2003).
39. K. Nordlund, J. Wallenius, and L. Malerba, *Nucl. Instruments Methods Phys. Res. Sect. B Beam Interact. Mater. Atoms* 246, 322 (2006).
40. C. Dimitrov, B. Sitaud, and O. Dimitrov, *J. Nucl. Mater.* 208, 53 (1994).
41. F. Gao and D.J. Bacon, *Philos. Mag. A* 67, 289 (1993).
42. B. Liu, F. Yuan, K. Jin, Y. Zhang, and W.J. Weber, *J. Phys. Condens. Matter* 27, 435006 (2015).
43. L.K. Béland, C. Lu, Y.N. Osetskiy, G.D. Samolyuk, A. Caro, L. Wang, and R.E. Stoller, *J. Appl. Phys.* 119, 85901 (2016).
44. M.W. Ullah, D.S. Aidhy, Y. Zhang, and W.J. Weber, *Acta Mater.* 109, 17 (2016).
45. L.K. Béland, Y.N. Osetsky, and R.E. Stoller, *Acta Mater.* 116, 136 (2016).
46. E. Levo, F. Granberg, C. Fridlund, K. Nordlund, and F. Djurabekova, *J. Nucl. Mater.* 490, 323 (2017).
47. E. Zarkadoula, G. Samolyuk, H. Xue, H. Bei, and W.J. Weber, *Scr. Mater.* 124, 6 (2016).
48. D.S. Aidhy, C. Lu, K. Jin, H. Bei, Y. Zhang, L. Wang, and W.J. Weber, *Acta Mater.* 99, 69 (2015).
49. S. Zhao, G. Velisa, H. Xue, H. Bei, W.J. Weber, and Y. Zhang, *Acta Mater.* 125, 231 (2017).
50. S. Zhao, Y.N. Osetsky, and Y. Zhang, *J. Alloys Compd.* 701, 1003 (2017).
51. S.I. Rao, C. Varvenne, C. Woodward, T.A. Parthasarathy, D. Miracle, O.N. Senkov, and W.A. Curtin, *Acta Mater.* 125, 311 (2017).
52. L.K. Béland, P. Brommer, F. El-Mellouhi, J.-F. Joly, and N. Mousseau, *Phys. Rev. E* 84, 46704 (2011).
53. H. Xu, Y.N. Osetsky, and R.E. Stoller, *Phys. Rev. B* 84, 132103 (2011).
54. L.K. Béland, Y.N. Osetsky, R.E. Stoller, and H. Xu, *J. Alloys Compd.* 640, 219 (2015).
55. G. Odette, B. Wirth, D. Bacon, and N. Ghoniem, *MRS Bull.* 26, 176 (2001).
56. P.R. Monasterio, B.D. Wirth, and G.R. Odette, *J. Nucl. Mater.* 361, 127 (2007).
57. G.S. Was, J.P. Wharry, B. Frisbie, B.D. Wirth, D. Morgan, J.D. Tucker, and T.R. Allen, *J. Nucl. Mater.* 411, 41 (2011).
58. L. Malerba, A. Caro, and J. Wallenius, *J. Nucl. Mater.* 382, 112 (2008).
59. D. Terentyev, G. Bonny, N. Castin, C. Domain, L. Malerba, P. Olsson, V. Moloddtsov, and R.C. Pasianot, *J. Nucl. Mater.* 409, 167 (2011).
60. G. Bonny, N. Castin, J. Bullens, A. Bakaev, T.C.P. Klaver, and D. Terentyev, *J. Phys. Condens. Matter* 25, 315401 (2013).